# Algorithm for an Estimation of the Electromagnetic Field Uniformity in the Working Volume of a Reverberation Chamber

Alexander V. Demakov, Maxim E. Komnatnov, *Member*, *IEEE*
Tomsk State University of Control Systems and Radioelectronics, Tomsk, Russia

***Abstract* – An analytical model for a rapid estimation of the distribution of the electromagnetic field in the working volume of a reverberation chamber (RC) with a rectangular enclosure is presented. The designed algorithm and software implementation of this model are described and an analysis of the non-uniform distribution of the *E*-field in the working volume of the RC with dimensions of 2.4×0.9×1.8 m$^3$ is performed. The analysis of the obtained results in the form of frequency dependences of the standard deviation of the components of the *E*-field strength is performed in accordance with IEC 61000-4-21.**

***Index Terms* – Reverberation chambers, mathematical model, electromagnetic compatibility, statistical analysis.**

## I. INTRODUCTION

ENSURING the electromagnetic compatibility (EMC) is an important task in the development of modern radioelectronic equipment (RE). The increase in the density of mounting of printed circuit boards, miniaturization and integration of the electronic component base lead to a decrease in the level of susceptibility of the RE to the electromagnetic field (EMF). Testing of electronic components and units for emission and radiated susceptibility is expensive because they require sophisticated measuring equipment (antennas, power amplifiers, generators, spectrum analyzers, etc.), as well as special anechoic chambers. The need for cheap test sets, while maintaining the adequacy of the results obtained with their help, leads to the search for alternative means for testing, one of which is the electromagnetic reverberation chamber (RC) [1].

Modern RC are developed using numerical methods, with the help of which it is possible to evaluate the main indicators of RCs quality at the design stage. Representation of an EMF in the form of a superposition of electromagnetic plane waves with a random direction of propagation allows simulating a stochastically uniform EMF in the RC. Thus, it was shown [2, 3] that with the use of a finite series of plane waves, selected on the basis of the theory of spectral samples, the process of numerical analysis can be accelerated with effective calculation of the currents induced on the object under test.

Approaches to the analysis of the distribution of EMF in the RC using the transmission-line matrix method are known [4]. It was revealed that the use of a hexagonal grid in the method, taking into account the rotation of stirrers in the model entails a sharp increase in the requirements for computing resources. To solve this problem, more specific methods are used, for example, the method based on image theory [5], which allows to evaluate the characteristics of the RC in both the time and frequency domains with lower requirements for computational resources. At the same time, at the preliminary stage of the RC development, it becomes necessary to obtain rough and fast estimates of the distribution of EMF at given frequencies.

The purpose of this work is to develop a software implementation of the model of the RC and to analyze the results obtained with its help.

## II. DESCRIPTION OF RC MODEL

The distribution of the EMF can be represented as a superposition of the modes excited inside the enclosure of the RC at a given frequency. The resonant frequencies of the excited modes for rectangular RC can be calculated using the expression for a rectangular resonator

$$f_{mnp} = \frac{c}{2}\sqrt{\left(\frac{m}{a}\right)^2 + \left(\frac{n}{b}\right)^2 + \left(\frac{p}{d}\right)^2} \qquad (1)$$

where $c$ is the speed of light in vacuum, $m, n, p$ are non-negative integers, $a, b$ and $d$ $(a < b < d)$ are the width, length and height of the rectangular cavity, respectively.

Each excited mode at frequency $f$ corresponds to the amplitude coefficient $I$, which is determined as a function of the calculated resonance frequency $f_{mnp}$ and quality factor $Q$ of RC [6]

$$I\left(f, f_{mnp}\right) = \frac{1}{\sqrt{1 + Q^2(f)\left(\frac{f}{f_{mnp}} - \frac{f_{mnp}}{f}\right)^2}} . \qquad (2)$$

The $Q$-factor determines the ratio of the energy of the EMF accumulated inside the shielded enclosure to the scattered energy throughout the cycle of mode stirring. The $Q$-factor in the high frequency range can be calculated as

$$Q = \frac{1}{{Q_w}^{-1} + {Q_{Rx}}^{-1} + {Q_{Tx}}^{-1}} .$$

978-1-7281-1753-9/19/$31.00 ©2019 IEEE

The quality factor $Q_w$, determined by the losses due to multiple reflections of the electromagnetic wave from the internal walls of the shielded enclosure, is calculated as

$$Q_w = \frac{3}{2}\frac{V}{\mu_r S \delta_w}\frac{1}{1+\frac{3\pi}{8k}\left(\frac{1}{a}+\frac{1}{b}+\frac{1}{d}\right)},$$

where $V$ is the internal volume of the shielded enclosure, $S$ is the area of the walls inside the shielded enclosure, $\mu_r$ is the relative magnetic permeability of air, $\delta_w$ is the thickness of the metal skin layer, $k$ is the wave number.

The components of quality factor $Q_{Rx}$ and $Q_{Tx}$, determined by the losses in the receiving ($Rx$) and transmitting ($Tx$) antennas, can be found by the following expressions:

$$Q_{Rx} = \frac{16\pi^2 \cdot V \cdot f^3}{m \cdot c^3},$$

$$Q_{Tx} = \frac{8\pi^2 \cdot V \cdot f^3}{m \cdot c^3}$$

where $m$ is the antenna matching factor.

Assuming that the electromagnetic wave propagates along the $z$-axis, rectangular components for $TE$ and $TM$ waves can be found from the expressions [7]

$$E_{x_{mnp}}^{TE^z} = \frac{-j\omega_{mnp}\mu k_y H_0}{k_{mnp}^2 - k_z^2}\cos k_x x \sin k_y y \sin k_z z, \quad (3)$$

$$E_{y_{mnp}}^{TE^z} = \frac{-j\omega_{mnp}\mu k_x H_0}{k_{mnp}^2 - k_z^2}\sin k_x x \cos k_y y \sin k_z z, \quad (4)$$

$$E_{z_{mnp}}^{TE^z} = 0, \quad (5)$$

$$E_{x_{mnp}}^{TM^z} = \frac{-k_x k_z E_0}{k_{mnp}^2 - k_z^2}\cos k_x x \sin k_y y \sin k_z z, \quad (6)$$

$$E_{y_{mnp}}^{TM^z} = \frac{-k_y k_z E_0}{k_{mnp}^2 - k_z^2}\sin k_x x \cos k_y y \sin k_z z, \quad (7)$$

$$E_{z_{mnp}}^{TM^z} = E_0 \sin k_x x \cos k_y y \sin k_z z. \quad (8)$$

The resulting EMF at frequency $f$ can be found as the superposition of fields excited by each resonant mode (1)-(2) within the range $f \pm \Delta f$, where $\Delta f = 100f / Q(f)$, taking into account (3)-(8):

$$E_i(f,x,y,z) = \sum_{f_{mnp} \in f \pm \Delta f} I(f, f_{mnp})\left(E_{i_{mnp}}^{TM^z} + E_{i_{mnp}}^{TE^z}\right),$$

where $i$ is the index of the $E$-field strength component ($x$, $y$ or $z$).

The model uses an infinitesimal isotropic source placed inside the enclosure of a RC. To account for the influence of the source location on the distribution of EMF the following coefficients are used [8]:

$$C_{x_{mnp}}^{TE^z} = \frac{-j\omega_{mnp}\mu k_y}{k_{mnp}^2 - k_z^2}\cos k_x x_e \sin k_y y_e \sin k_z z_e,$$

$$C_{x_{mnp}}^{TM^z} = \frac{-k_x k_z}{k_{mnp}^2 - k_z^2}\cos k_x x_e \sin k_y y_e \sin k_z z_e,$$

where $x_e$, $y_e$, $z_e$ are the coordinates of the location of the source inside the enclosure.

Thus, the expression for calculating the $i$-components of the $E$-field strength takes the form

$$E_i = \sum_{f_{mnp} \in f \pm \Delta f} I(f, f_{mnp})\left(C_{i_{mnp}}^{TM^z} E_{i_{mnp}}^{TM^z} + C_{i_{mnp}}^{TE^z} E_{i_{mnp}}^{TE^z}\right).$$

## III. SOFTWARE IMPLEMENTATION OF RC MODEL

Initially, the model was developed in the Octave software [9]. The frequency dependences of the amplitude of the absolute value of the $E$-field strength at the center of the RC's shielding enclosure with a size of 1.2×1.7×2.1 m$^3$ with changing frequency sweep step $\Delta f_s$ were calculated. The analysis of the obtained results revealed that the correct description of the $E$-field inside the RC in the low-frequency region (about 100-400 MHz) is achieved with values of $\Delta f_s$ not exceeding 1 MHz. At the same time, the decrease in $\Delta f_s$ leads to a significant increase in the computation time: when $\Delta f_s$ decreases from 50 MHz to 5 MHz, time costs increase 32.38 times (7935 s), and from 5 MHz to 1 MHz - 42.57 times (332047 s). To reduce time costs, the model was implemented in C++ language using libraries for organizing multithreading and storing the results of calculations in spreadsheet format. The algorithm of the developed program is presented in Fig. 1.

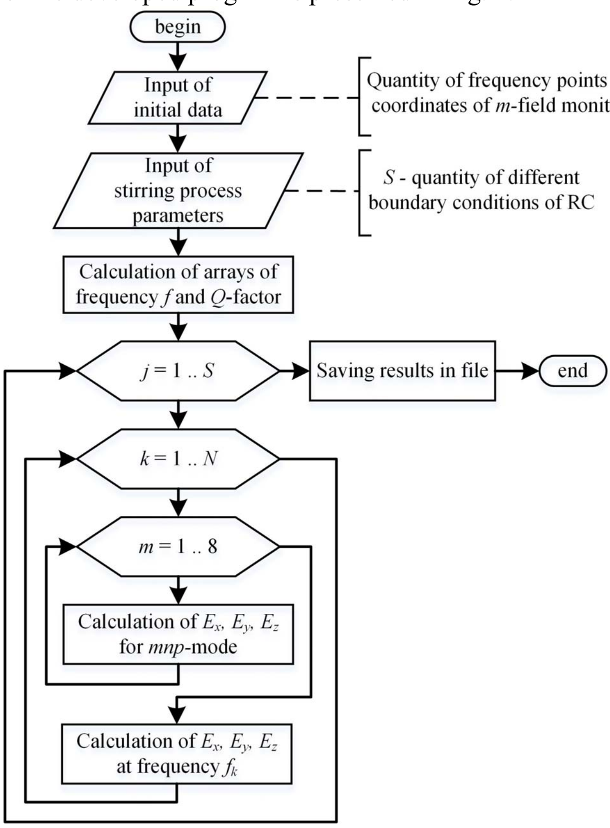


Fig. 1. Algorithm of software implementation for the RC model

At the first step, the program performs initialization of the source data and parameters responsible for changing the boundary conditions of the RC. Next, the array of frequency points and the frequency dependence of the *Q*-factor of the RC is calculated, after which, for each boundary condition, the frequency dependences of the rectangular components of the *E*-field intensity are calculated.

## IV. RESULTS OF SIMULATION

### A. Initial data

For the development of the RC, a shielding enclosure with dimensions of $2.4{\times}0.9{\times}1.8$ m$^3$ was taken. According to [10], the EMF non-uniformity in the RC is determined using direct measurements of the *E*-field strength at 8 points that define the boundaries of the working volume. In this case, the *E*-field monitors should be located at a distance of at least $\lambda_{LUF}/2$ ($\lambda_{LUF}$ - the wavelength corresponding to lower usable frequency of RC) from the walls of the enclosure, stirrers and antennas. Based on these requirements, the lower usable frequency $f_{LUF} = c / \lambda_{LUF}$ was selected equal to 600 MHz.

The working volume of the RC ($0.9{\times}0.3{\times}1.0$ m$^3$) and the coordinates of the isotropic source (*x*=0.2 m; *y*=0.4 m; *z*=0.2 m) were determined based on the geometric parameters of the enclosure and $\lambda_{LUF}$. The coordinates of the *E*-field monitors are summarized in Table I.

TABLE I
COORDINATES OF THE E-FIELD MONITORS

| No. of field monitor | *x*, m | *y*, m | *z*, m |
|---|---|---|---|
| 1 | 1.1 | 0.3 | 1.4 |
| 2 | 1.1 | 0.3 | 0.4 |
| 3 | 1.1 | 0.6 | 1.4 |
| 4 | 1.1 | 0.6 | 0.4 |
| 5 | 2 | 0.3 | 1.4 |
| 6 | 2 | 0.3 | 0.4 |
| 7 | 2 | 0.6 | 1.4 |
| 8 | 2 | 0.6 | 0.4 |

For the given initial data, the frequency dependences of the *Q*-factor (Fig. 2) and the number of excited modes (Fig. 3) are calculated at 45 frequency points in the range from 600 to 2000 MHz. For small-sized RCs, *Q*-factor is $\approx 10^3$ at frequencies up to 1 GHz, and more than $10^3$ at high frequencies [11], which corresponds to the calculated frequency dependence (Fig. 2). From [12] it is known that in order to achieve a uniform distribution of EMF, it is necessary to excite at least 60 modes at a given frequency. As can be seen from Fig. 3, 62 modes are excited inside the RC at the lower boundary frequency. The number of modes increases with increasing the frequency, which satisfies the conditions of [12].

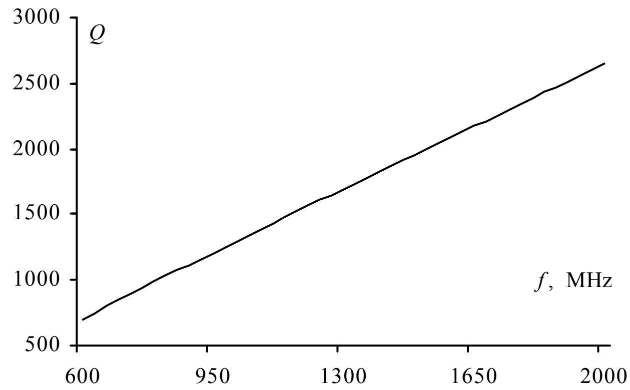


Fig. 2. The frequency dependence of the quality factor *Q*

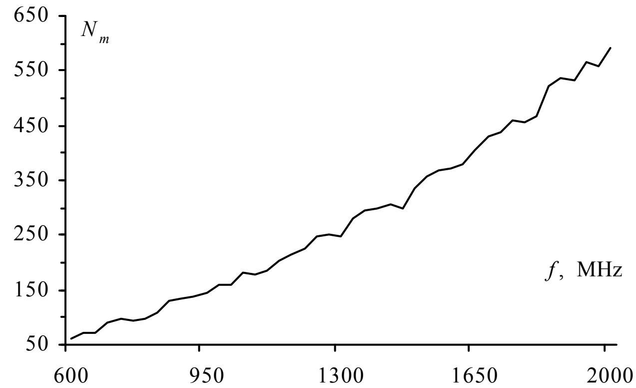


Fig. 3. The frequency dependence of the number of excited modes $N_m$

### B. Modeling of the mode stirring process

The simulation of RC with electronic stirring of modes was performed using the developed software. The change of the boundary conditions for the propagation of electromagnetic waves in the RC was carried out using spatial movement (change of coordinates) of the source along the polygonal and linear paths (Fig. 4). The coordinates of the source as it moves along a polygonal and linear paths are presented in Table II.

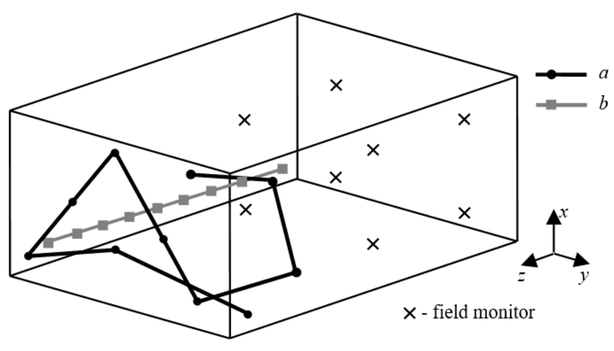


Fig. 4. Polygonal (*a*) and linear (*b*) paths of the source movement in the RC

TABLE II
THE COORDINATES OF THE SOURCE AS IT MOVES ALONG A POLYGONAL AND LINEAR PATHS

| № of source position | x, m | | y, m | | z, m | |
|---|---|---|---|---|---|---|
| | *a* | *b* | *a* | *b* | *a* | *b* |
| 1 | 0.08 | 0.3 | 0.74 | 0.1 | 1.25 | 0.2 |
| 2 | 0.12 | 0.3 | 0.78 | 0.1425 | 1.62 | 0.28875 |
| 3 | 0.44 | 0.3 | 0.7 | 0.185 | 1.5 | 0.3775 |
| 4 | 0.54 | 0.3 | 0.12 | 0.27 | 1.5 | 0.555 |
| 5 | 0.14 | 0.3 | 0.1 | 0.355 | 1.11 | 0.7325 |
| 6 | 0.02 | 0.3 | 0.4 | 0.44 | 0.95 | 0.91 |
| 7 | 0.24 | 0.3 | 0.7 | 0.525 | 0.4 | 1.0875 |
| 8 | 0.2 | 0.3 | 0.1 | 0.61 | 0.2 | 1.265 |
| 9 | 0.58 | 0.3 | 0.08 | 0.695 | 0.32 | 1.4425 |
| 10 | 0.54 | 0.3 | 0.02 | 0.78 | 1.01 | 1.62 |

### C. Analysis of simulation results

The rectangular components of the *E*-field strength are calculated at the nodal points of the working volume of the RC in the frequency range 600-2000 MHz. The analysis of field uniformity was performed according to the method presented in the ESA manual [12]. At a fixed frequency for each field monitor, the maximum value of each component of the *E*-field is determined for all positions of the source ($\varphi_j = \varphi_1, ..., \varphi_N$)

$$\widetilde{E}_{\alpha,i} = \max_{\varphi_j=\varphi_1,...,\varphi_N} \left|E_\alpha(r_i)\right|_{\varphi_j} \quad (9)$$

where α is the index of the rectangular component of the *E*-field, *j* is the index of the position of the source, $i = 1, 2, ... 8$ is the number of *E*-field monitor.

The arithmetic mean of the maximum *E*-field from all measurements can be calculated as

$$\left\langle \widetilde{E}_\alpha \right\rangle = \frac{1}{8}\sum_{i=1}^{8} \widetilde{E}_{\alpha,i} \; . \quad (10)$$

The standard deviation for each rectangular component of *E*-field can be found as

$$\sigma_\alpha = \sqrt{\frac{\sum_{i=1}^{8}\left(\widetilde{E}_{\alpha,i} - \left\langle \widetilde{E}_\alpha \right\rangle\right)}{8-1}} \; . \quad (11)$$

The standard deviation expressed in decibels is defined as

$$\sigma_{\alpha_{dB}} = 20\log_{10}\frac{\sigma_\alpha + \left\langle \widetilde{E}_\alpha \right\rangle}{\left\langle \widetilde{E}_\alpha \right\rangle} \; . \quad (12)$$

The frequency dependences of the standard deviation of the rectangular components of the *E*-field strength were calculated according to (9)-(12) when moving the impact source along a polygonal (Fig. 5 *a*) and linear (Fig. 5 *b*) paths.

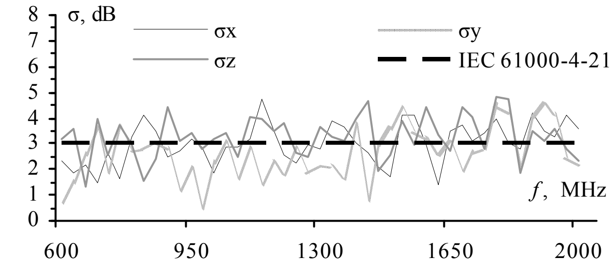


a

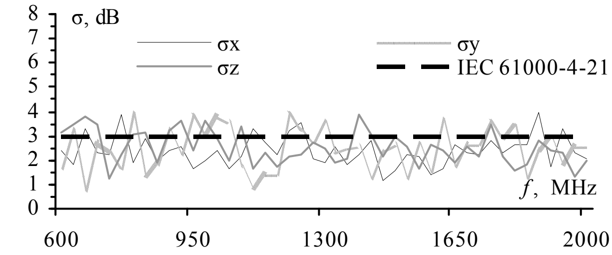


b

Fig. 5. The frequency dependences of the standard deviation of the calculated rectangular components of the *E*-field when moving the source along the polygonal (*a*) and linear (*b*) paths

When moving the source along a polygonal path (Fig. 5 *a*), the maximum σ value is 4.8 dB, which exceeds the set limit by 1.8 dB, according to [13]. However, with a linear path of movement of the source (Fig. 5 *b*), the maximum value of σ exceeds the limit set by the standard by 1 dB.

The high level of non-uniformity of the *E*-field can be caused by a small sample size of the calculated *E*-field, since the calculations made at 10 different source positions were taken into account when calculating the standard deviation. In the future, it is planned to improve software implementation to simulate the mechanical mode stirring process and to take into account the power supplied to the input of the antenna.

## V. CONCLUSION

A software implementation of the RC model, which is necessary for a rapid estimate of the distribution of EMF, is presented. The standard deviation of the rectangular components of the *E*-field strength in the working volume of the RC with dimensions of $2.4\times0.9\times1.8\ m^3$ was calculated to simulate the mode stirring process by moving the source. Analysis of the obtained results revealed their satisfactory convergence with the requirements of the IEC 61000-4-21 standard.

## ACKNOWLEDGMENT

This research was supported by The Ministry of Education and Science of the Russian Federation (RFMEFI57417X0172).

## REFERENCES


[1] A. V. Demakov, M. E. Komnatnov, T. R. Gazizov, "Review of research in the development and application of reverberation chambers for electromagnetic compatibility tests", *Systems of Control, Communication and Security*, 2018, no. 2, pp. 151-190. Available at: http://sccs.intelgr.com/archive/2018-02/09-Demakov.pdf (in Russian).

[2] J. C. West, C. F. Bunting, V. Rajamani, "Accurate and efficient numerical simulation of the random environment within an ideal reverberation chamber", *IEEE Transactions on Electromagnetic Compatibility*, vol. 54, no. 1, pp. 167-173, Feb. 2012.

[3] D. A. Hill, J. M. Ladbury, "Spatial-correlation functions of fields and energy density in a reverberation chamber", *IEEE Transactions on Electromagnetic Compatibility*, vol. 44, no. 1, pp. 95-101, Feb. 2002.

[4] A. Coates, H. G. Sasse, etc., "Validation of a three-dimensional transmission line matrix (TLM) model implementation of a mode-stirred reverberation chamber", *IEEE Transactions on Electromagnetic Compatibility*, vol. 49, no. 4, pp. 734-744, Nov. 2007.

[5] E. Amador, C. Lemoine, etc., "Reverberation chamber modeling based on image theory: investigation in the pulse regime", *IEEE Transactions on Electromagnetic Compatibility*, vol. 52, no. 4, pp. 778-789, Nov. 2010.

[6] F.E. Terman, "Radio Engineer's Handbook", NY: McGraw-Hill Book Company, 1943.

[7] D.A. Hill, "Electromagnetic Fields in Cavities: Deterministic and Statistical Theories". Hoboken, NJ: John Wiley & Sons, Inc., 2009.

[8] E. Amador, P. Besnier, "Source stirring analysis in a reverberation chamber based on modal expansion of the electric field", *IEEE Int. Symp. on Electromagn. Compat.*, pp. 434-439, 16–22, Aug. 2015.

[9] E.A. Safronova, A.M. Artjushkina, A.V. Demakov, "Testirovanie programmnoj realizacii analiticheskoj modeli reverberacionnoj kamery" [Testing the software implementation of the analytical model of the reverberation chamber], Nauchnaja sessija TUSUR–2018, Tomsk, Russia, 2018, pp. 235-237 (In Russian).

[10] Space engineering. Electromagnetic compatibility handbook. – ESA Requirements and Standards Division, ESTEC, 2012, 228 p.

[11] Y. Cui, G. Wei, etc., "Fast calculation of reverberation chamber Q-factor", *Electronics Letters*, vol. 48, no. 18, pp. 1116-1117, 30 Aug. 2012.

[12] K. Malarić, K. Košutić, "Design and construction of a small reverberation chamber", *International Journal of Electrical and Computer Engineering Systems*, vol. 7, no. 2, pp. 47-51, 2016.

[13] *Electromagnetic compatibility (EMC), Part 4-21: Testing and measurement techniques – Reverberation chamber test methods*, IEC 61000-4-21, 2011.


**Alexander V. Demakov** was born in 1994. He graduated from the TUSUR in 2018. Currently, he works as a junior researcher at the Research Laboratory «SECRF» and is studying at the postgraduate programm of TUSUR. The field of scientific interests is development of EMC test facilities.

**Maxim E. Komnatnov** was born in 1987. He graduated from the TUSUR in 2013. He defended his Ph.D. thesis. Currently, he works as a senior researcher at the Research Laboratory «SECRF» and an associate professor at the Department of TUSUR. The field of scientific interests is measurements and tests on EMC. M.E. Komnatnov is the author of 91 scientific works.